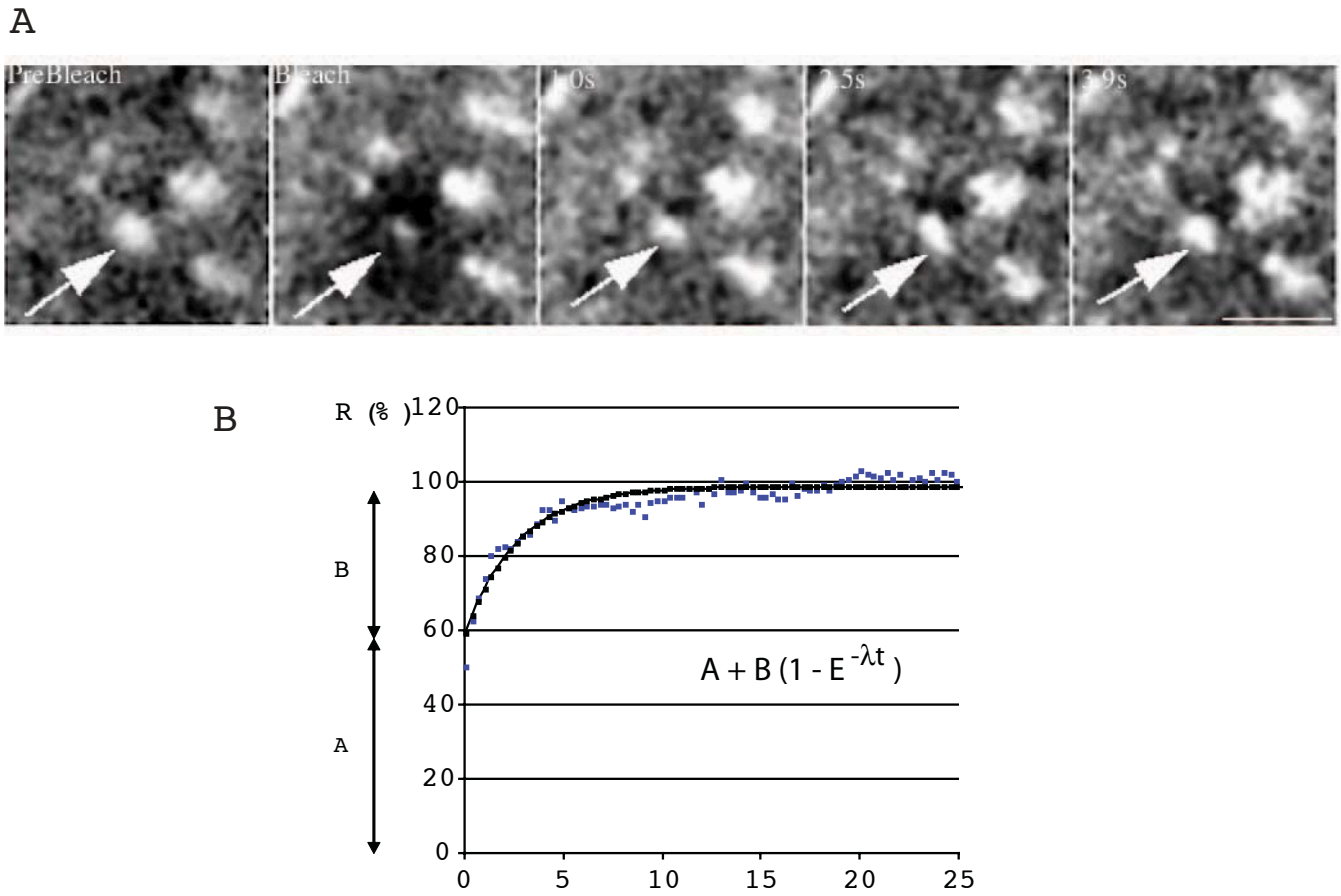

Figure S1 FRAP analysis of COPII turnover on the ER. Vero cells were microinjected with constructs encoding FP-COPII. FRAP was performed as described in supplementary methods. **A**: an example of photobleaching a single COPII labelled ERES. Only YFP-Sec23Ap is shown. Panels indicate before and after photobleaching. The arrow indicates the bleached ERES. No bleaching of the other YFP-Sec23Ap labelled ERES is observed. Time is seconds after bleaching. Scale Bar, 1 m. **B:** the recovery curve for a typical FRAP experiment. Data is from a single experiment with YFP-Sec31Ap being photobleached, raw data is in blue, the fit of the data to a single exponential recovery function (equation shown) is in black.. A is the extent of bleaching, B is the amount of recovery, and λ is related to $t_{1/2}$ by $t_{1/2} = \ln 0.5/\lambda$. R (%) is the percent of recovery relative to the original fluorescence before photobleaching. Time is in seconds.

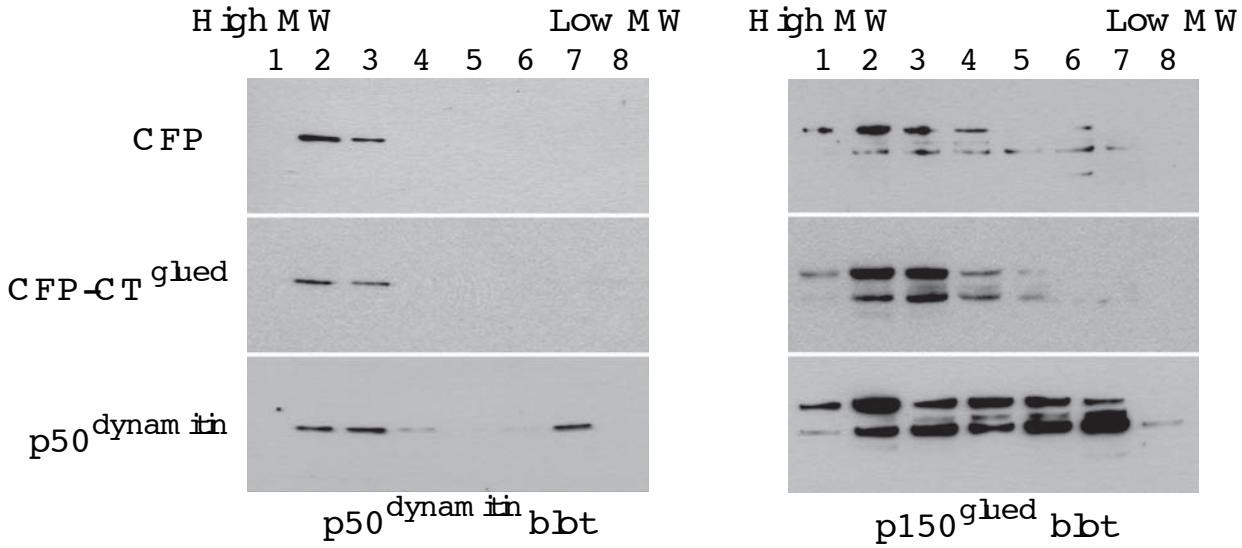

Figure S2 Sedimentation analysis. Lysates were prepared from cells expressing CFP, CFP-CT^{Glued} or p50^{dynamitin} and sedimented on 5-20% sucrose gradients. Fractions were then immunoblotted for p50^{dynamitin} or p150^{Glued}. Note that the antibody used for detection of p50^{dynamitin} does not recognize the transfected chick p50^{dynamitin} protein (data not shown). Note also the presence of p50^{dynamitin} and p150^{Glued} in cells expressing p50^{dynamitin} but not those expressing CFP or CFP-CT^{Glued}. Expression of p50^{dynamitin} causes dissociation of the dynactin complex and both p50^{dynamitin} itself and p150^{glued} are displaced from the dynactin complex (appearing in the lower molecular mass fractions of the sucrose gradient, concentrated in fraction 7, note that the antibody used for detection of p50^{dynamitin} does not recognize the transfected chick p50^{dynamitin} protein, only the endogenous, human, protein (data not shown). In contrast, expression of CFP-CT^{glued} does not cause this dissociation and p50^{dynamitin} and p150^{glued} immuno-reactivity remains associated with high molecular mass fractions.

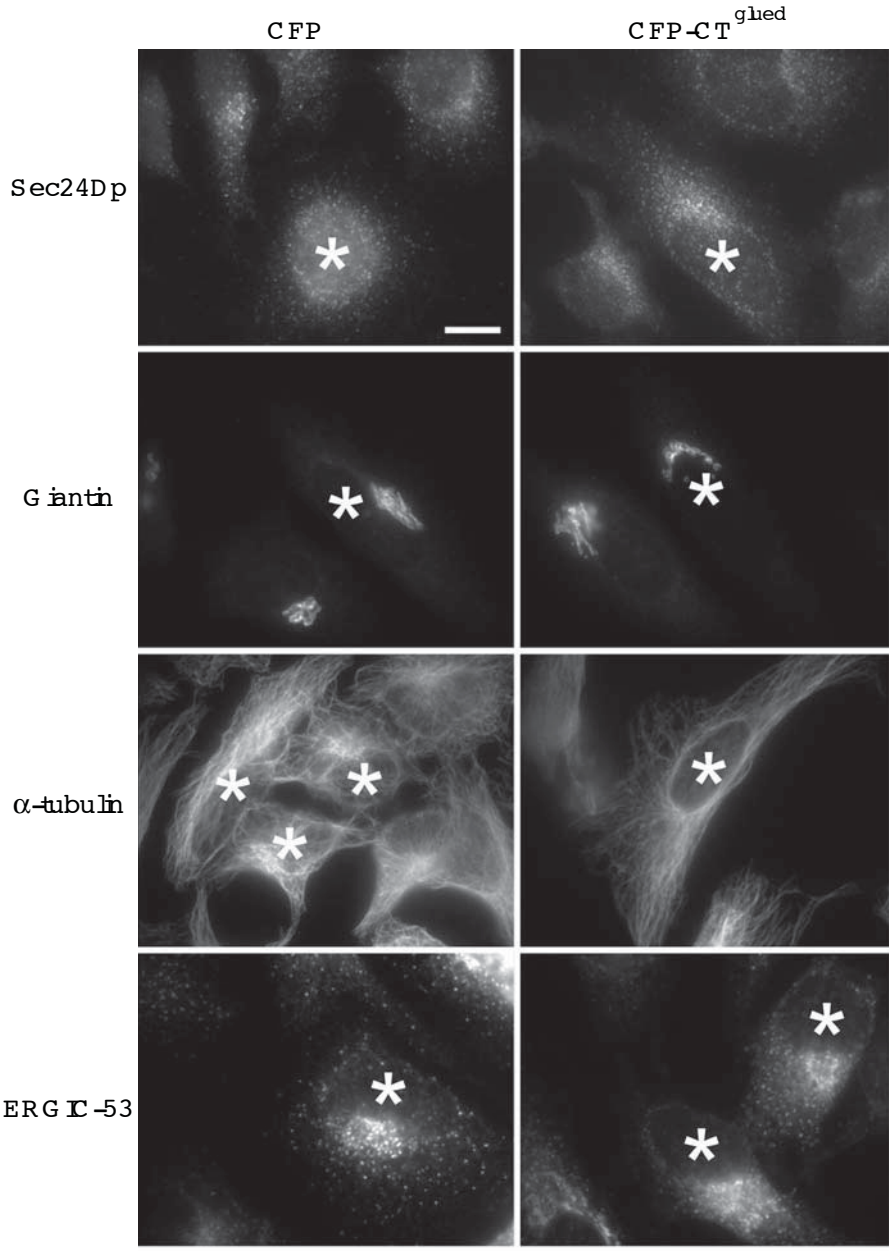

Figure S3 Effect of CT^{glued} expression on organization of the early secretory pathway. HeLa cells transfected with either CFP or CFP-CT^{glued} were fixed and processed for immunofluorescence using antibodies against Sec24Dp (COPI), giantin (Golgi), tubulin (microtubules) and ERGIC-53 (VTCs and other ER-Golgi transport intermediates). Asterisks indicate transfected cells. This expression level of CFP and CFP-CT^{glued} was used for all experiments described. Bar = 10 m. In cells expressing CFP-CT^{glued} the localization of Sec24Dp was not significantly disrupted, nor was the localization of α-tubulin (at this level of expression of CFP-CT^{glued}). Furthermore, CFP-CT^{glued} did not cause significant fragmentation of the Golgi apparatus (giantin localization). Localization of ERGIC-53, which cycles constitutively between the ER and Golgi, was slightly disrupted, becoming less concentrated in the juxta-nuclear (Golgi) region in cells expressing CFP-CT^{glued} but not those expressing CFP.

Movie 1 Cells expressing YFP-Sec23Ap were microinjected with rhodamine-tubulin and analyzed by time-lapse microscopy. The movie pauses at certain points to highlight associated structures. A red arrowhead highlights the end of one growing microtubule with white arrowheads highlighting ERES which rapidly associate with this newly polymerised microtubule.
Movie 2 Cells co-expressing GFP-Sec23Ap and GFP-p150^{Glued} were imaged using wide-field time-lapse microscopy. Note that p150^{Glued}-positive microtubule plus ends encounter static ERES in the cytoplasm. This is most evident over the nucleus of the cell where contrast is highest. Bar = 10 m.
Movie 3 Enlarged region of movie 2 showing the area above the nucleus. Note the mobile GFP-p150^{Glued}–labelled microtubule plus ends pass in direct proximity to ERES.
Movie 4 Two whole cell movies running simultaneously at equal frame rates show the delayed export and transport to the Golgi of ts045-G-YFP in cells expressing CFP-CT^{Glued} (lower panel) compared to those expressing CFP alone (upper panel). Note the difference in time of the appearance of VTCs in the cytoplasm and localization of fluorescent cargo to the Golgi. Bar = 10 m.
Movie 5 Two movies running simultaneously at equal frame rates show the delayed formation of ts045-G-YFP containing transport carriers in cells expressing CFP-CT^{Glued} (right-hand panel) compared to those expressing CFP alone (left-hand panel). Bar = 10 m.

SUPPLEMENTARY METHODS

Fluorescence Recovery After Photobleaching (FRAP). Vero cells were microinjected with constructs encoding YFP and CFP COPII subunits, and then imaged in carbonate free imaging medium using an LSM510 confocal microscope (Zeiss) fitted with a 413nm Kr and 488 and 514nm argon ion laser lines, using a 63x PlanApochromat NA 1.4 DIC oil immersion objective. Cells were imaged using 413nm-514nm line switching and 5 pre-bleach images were taken. An area of 5% of the cell was imaged and a single ER exit site in this area was then bleached, representing approximately 0.1% of the total cell area. The bleaching area encompassing a single ER exit site was maintained constant during all experiments. Bleaching was adjusted to about 50% of the pre-bleach fluorescence intensity, using 100% laser power of the 514nm (YFP only) laser line for 0.5s (5 iterations). Subsequently, recovery was observed, using 1% laser power with time intervals between images of 0.3s for 90 frames. The data was treated to low pass 3x3 filtering using the LSM510 software (Zeiss) to reduce image noise. CFP and YFP sequences were then exported as TIFF sequences using the LSM510 software. Recovery data was subsequently loaded into a macro designed in Interactive Data Language (IDL 5.3, Research Systems Inc., Boulder Co.). The macro thresholded images in order to eliminate background fluorescence. Data was then corrected for bleaching, by dividing the fluorescence intensity of the bleached area by that of an unbleached area. Bleaching was minimal during the time course of recovery, between 0-10% and where more bleaching was observed, the recovery sequences were discarded. Finally the corrected YFP and CFP images were divided by each other. Recovery data was then entered into Mathematica 3.0 (Wolfram Research). Where the recovery data was fitted to the equation (1) from which the half time for recovery, $t_{1/2}$, was calculated.

$$A + B\,(1 - E^{-\lambda t}) \quad (1)$$

Where A = fluorescence directly after photobleaching (%), B = mobile fraction, (is related to $t_{1/2}$ by the equation, $t_{1/2} = \ln 0.5/\lambda$

Table 1 Turnover of COPII subunits at ER exit sites

GFP–COPII	Treatment	*n*	$t_{1/2}$ (s)
Sec23Ap	none	18	4.0 ± 0.3
	CFP-CT^{Glued}	12	1.6 ± 0.4
	p150^{Glued}	12	1.5 ± 0.6
	p50^{dynamitin}	11	1.9 ± 0.2
	nocodazole (1 hour)	6	2.6 ± 0.2
Sec31Ap	none	29	3.1 ± 0.1
	CFP-CT^{Glued}	5	1.5 ± 0.3
	p150^{Glued}	5	2.1 ± 0.5
	p50^{dynamitin}	8	0.8 ± 0.1
	nocodazole (1 hour)	5	1.9 ± 0.4

Vero cells were injected with constructs encoding FP-COPII subunits as described in materials and methods. For nocodazole treatment, samples were treated with 10μM nocodazole for 60 minutes. Constructs encoding p50^{dynamitin}, p150^{Glued} or CFP-CT^{Glued} were co-microinjected with constructs encoding FP-COPII, as described in materials and methods. *n* = number of cells measured. Further details of these experiments are included as supplementary material.